

On the extended stellar structure around NGC 288

Andrés E. Piatti^{1,2*}

¹*Consejo Nacional de Investigaciones Científicas y Técnicas, Av. Rivadavia 1917, C1033AAJ, Buenos Aires, Argentina*

²*Observatorio Astronómico, Universidad Nacional de Córdoba, Laprida 854, 5000, Córdoba, Argentina*

Accepted XXX. Received YYY; in original form ZZZ

ABSTRACT

We report on observational evidence of an extra-tidal clumpy structure around NGC 288 from an homogeneous coverage of a large area with the Pan-STARRS PS1 database. The extra-tidal star population has been disentangled from that of the Milky Way field by using a cleaning technique that successfully reproduced the stellar density, luminosity function and colour distributions of MW field stars. We have produced the cluster stellar density radial profile and a stellar density map from independent approaches, from which we found results in excellent agreement : the feature extends up to 3.5 times the cluster tidal radius. Previous works based on shallower photometric data sets have speculated on the existence of several long tidal tails, similar to that found in Pal 5. The present outcome shows that NGC 288 could hardly have such tails, but favours the notion that interactions with the MW tidal field has been a relatively inefficient process for stripping stars off the cluster. These results point to the need of a renewed overall study of the external regions of Galactic globular clusters (GGCs) in order to reliably characterise them. Hence, it will be possible to investigate whether there is any connection between detected tidal tails, extra-tidal stellar populations, extent diffuse halo-like structures with the GGCs' dynamical histories in the Galaxy.

Key words: techniques: photometric – (Galaxy:) globular clusters: individual (NGC 288)

1 INTRODUCTION

A non-negligible number of Galactic globular clusters (GGCs) have shown extended stellar structures around them (Carballo-Bello et al. 2012). For instance, an extended stellar halo surrounding the distant NGC 5694 was discovered by Correnti et al. (2011), while an unprecedented extra-tidal, azimuthally smooth, halo-like diffuse spatial extension of NGC 1851 was found by Olszewski et al. (2009). Piatti (2017a) also found a similar feature around 47 Tuc. Other GGCs were found to be embedded in a diffuse stellar envelope extending to a radial distance of at least five times the nominal tidal radius, like M 2 (Kuzma et al. 2016); and long tidal tails have been detected in the field of Pal 5 (Odenkirchen et al. 2003), Pal 14 (Sollima et al. 2011), Pal 15 (Myeong et al. 2017), and NGC 7492 (Navarrete et al. 2017). As far as theoretical developments are considered, some N-body experiments have shown that the detection of extended envelopes around GGCs could be due to potential escapers (Küpper et al. 2010) or potential observational biases (Babinot & Gieles 2017), among others.

As far as NGC 288 is considered, Leon et al. (2000) used

photographic photometry to claim that the cluster has very important tidal tails extending up to 350 pc from its centre. They noticed that NGC 288 had been previously observed by Grillmair et al. (1995), who found tidal extensions on a field 200' × 200' smaller than theirs, but with the same spatial resolution (16'). Leon et al. (2000) showed that their wavelet decomposition clearly reveals some wide structures missed by Grillmair et al. (1995), especially towards the south. Particularly, they highlighted two main tidal tails, one running from the cluster centre towards the south-east (parallel to the cluster proper motion vector, PA ≈ 51°; Dinescu et al. 1997) and another one towards the Galactic centre (PA ≈ 140°). They also mentioned that the photometric error at $B \sim 20.0$ mag is $\sigma(B) \sim 0.2$ mag and that Abell galaxy clusters affect their surface densities built using a *Gaussian* kernel of 16 arcmin, which is similar to the size of the cluster tidal radius (Trager et al. 1993; Grillmair et al. 1995; Harris 1996; Miocchi et al. 2013).

Later, Grillmair et al. (2004) speculated on the existence of a long tidal tail of 8.5° from the cluster centre towards the north-west – that Leon et al. (2000) did not detect – beside its counterpart tail of 8.5° to the south-east. They used 2MASS data that barely reaches the horizontal branch of the cluster. According to Gnedin & Ostriker

* E-mail: andres@oac.unc.edu.ar

(1997) and [Dinescu et al. \(1999\)](#), NGC 288 has experienced disruption by tidal shocks more important than by internal relaxation and evaporation, so that tidal tails should be expected as debris from those interactions with the Milky Way (MW). Multiple tidal tails from the interaction with the MW potential have also been recently predicted from numerical simulations ([Hozumi & Burkert 2015](#)), while [Balbinot & Gieles \(2017\)](#) have pointed out that NGC 288 is one of the GGCs with the optimal detectability conditions of tidal tails, namely, a low remaining mass fraction μ - which is a measure of its stage of dissolution -, and a high orbital phase ϕ . [Dinescu et al. \(1999\)](#) listed other seven GGCs with similar dynamical histories as NGC 288, Pal 5 being the only one with confirmed long tidal tails ([Odenkirchen et al. 2001, 2003; Erkal et al. 2017](#)). The other six clusters do not show any observational hints for such a structure ([Chen & Chen 2010](#)).

In this paper we show from deep wide-field photometry that NGC 288 exhibits a single extra-tidal cumply structure, as commonly seen in other GGCs (e.g. [Grillmair et al. 1995; Chen & Chen 2010; Piatti 2017a](#)), no evidence of long tails is detected. Section 2 deals with the description of the database used, while Sections 3 and 4 focus on independent approaches to produce the cluster stellar density radial profile and a stellar density map of its outskirts. In Section 5 we discuss the outcomes to the light of previous results and pose further studies that will be possible the address from upcoming releases of ongoing surveys. Finally, Section 6 summaries the main conclusions of this work.

2 OBSERVATIONAL DATA

In order to clearly identify and trace tidal tails in the field of NGC 288, we need to cover homogeneously a large sky area centred on the cluster with deep photometry. For this purpose, we made use of the public astrometric and photometric catalogue produced by the Panoramic Survey Telescope and Rapid response System (Pan-STARRS PS1¹; [Chambers et al. 2016](#)). We downloaded positions (R.A. and Dec.) and gr PSF photometry for 316984 stars distributed in a box of $4^\circ \times 4^\circ$ centred on NGC 288. Aiming at illustrating this wealth of information, Fig. 1 depicts the intrinsic colour-magnitude diagram (CMD) of the inner cluster region ($r < 5$ arcmin (12.9 pc)) and that of a same area star field

¹ The Pan-STARRS1 Surveys (PS1) and the PS1 public science archive have been made possible through contributions by the Institute for Astronomy, the University of Hawaii, the Pan-STARRS Project Office, the Max-Planck Society and its participating institutes, the Max Planck Institute for Astronomy, Heidelberg and the Max Planck Institute for Extraterrestrial Physics, Garching, The Johns Hopkins University, Durham University, the University of Edinburgh, the Queen's University Belfast, the Harvard-Smithsonian Center for Astrophysics, the Las Cumbres Observatory Global Telescope Network Incorporated, the National Central University of Taiwan, the Space Telescope Science Institute, the National Aeronautics and Space Administration under Grant No. NNX08AR22G issued through the Planetary Science Division of the NASA Science Mission Directorate, the National Science Foundation Grant No. AST-1238877, the University of Maryland, Eotvos Lorand University (ELTE), the Los Alamos National Laboratory, and the Gordon and Betty Moore Foundation.

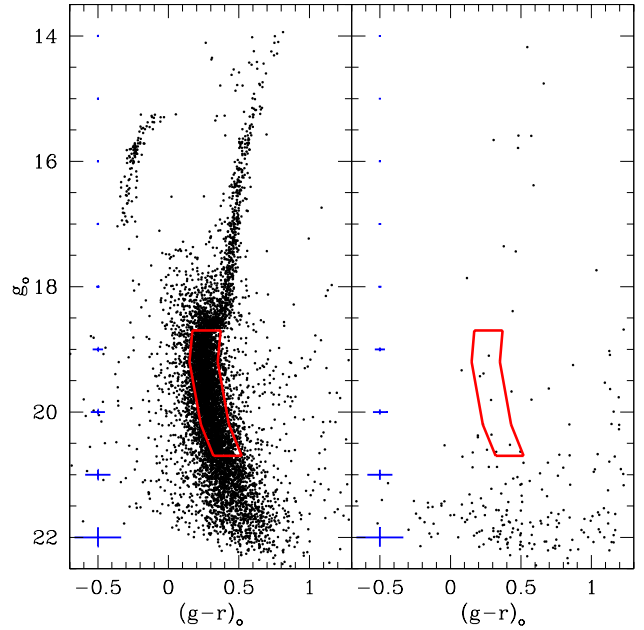


Figure 1. Colour-magnitude diagrams of stars in the field of NGC 288 ($r < 5$; left panel) and in a same area MW field located ~ 1.5 degree towards north-east (right panel). Errorbars are included at the left margin of each panel (blue lines). The region used to perform star counts is overplotted with a red contour line.

located ~ 1.5 degree towards the north-east. To derive intrinsic magnitudes g_0 and colours $(g-r)_0$ we corrected the Pan-STARRS PS1 gr magnitudes by interstellar absorption using the $E(B-V)$ values of each individual star obtained from [Schlafly & Finkbeiner \(2011\)](#), which is the recalibrated Milky Way (MW) extinction map of [Schlegel et al. \(1998\)](#). The average colour excess for the whole surveyed field is $E(B-V) = 0.014 \pm 0.001$ mag. This means that the sky area used in this analysis is affected by a low colour excess with no sign of differential reddening.

3 STAR COUNTS

To trace the cluster stellar density radial profile and to build the stellar density map of the analysed region, we considered stars along a strip of the cluster main sequence (MS), from its main sequence turnoff (MSTO) down to 2 mags, as is depicted with red lines in Fig. 1. It expands g_0 magnitudes and $(g-r)_0$ colours in the range (18.7,20.7) and (0.15,0.52), respectively. Notice that the strip was traced using stars within 5 arcmin (12.9 pc) of the NGC 288's centre, where more of them are probably cluster members. This assumption is particularly supported by the fact that the same region in the CMD for any MW field located well beyond the cluster body does not seem to contain so many stars (see Fig. 1). The selected stars, because of their smaller masses, can be found far away from the cluster main body ([Carballo-Bello et al. 2012](#), and references therein), and have been used previously for searching extra-tidal structures in different GGCs (see, e.g. [Olszewski et al. 2009; Saha et al. 2010; Piatti 2017a](#)). We decided to go as deep as to be within 100 per cent of the

Table 1. Positions and covered areas of control fields.

Method	Relative R.A.cos(Dec.) (deg)	Relative Dec. (deg)	size (deg ²)
Star counts	-2.0 to 2.0	1.5 to 2.0	4.0×0.5
	-2.0 to -1.5	-2.0 to 1.5	0.5×3.5
	-1.75	1.75	0.5×0.5
CMD cleaning	1.75	1.75	0.5×0.5
	1.75	-1.75	0.5×0.5
	-1.75	-1.75	0.5×0.5

photometry completeness; the 50 per cent photometry completeness being at $g=r=23.2$ mag, determined with PSF photometry of stellar sources in the stacked images (Farrow et al., in preparation).

To count stars distributed throughout the surveyed region and within the defined MS strip, we first split the total analysed field in small adjacent boxes of $0.10^\circ \times 0.10^\circ$ that covered the entire area. Then, we counted the number of MS strip stars inside them and computed the mean stellar density as a function of radius by averaging the star counts in every box placed within rings centred on the cluster of radius r and $r+\Delta(r)$. Thus, we also estimated an uncertainty in stellar counts due to stellar fluctuations in each ring. We repeated this exercise with boxes of increasing size in steps of 0.01° per side, up to $0.20^\circ \times 0.20^\circ$. On the other hand, we also considered that a star can fall outside the MS strip because of its photometric errors (see errorbars in Fig. 1), and thus change the total number of stars within the MS strip. Notice that this is not an issue of incompleteness in the photometry, since we decided to use stars brighter than the magnitude at the 100 per cent of photometry completeness. We then averaged all the generated individual stellar density radial profiles, and the resultant one is depicted in Fig. 2 (left panel) with black open circles. We have considered outer cluster regions where the Pan-STARRS PS1 data set is at a 100 per cent completeness level.

The background level was estimated using a relatively large area embracing the surveyed one (see Table 1) from which we computed the mean and standard deviation values. The resultant dispersion takes into account spatial variation of MW field stars distribution in the MS strip. As can be seen in Fig. 2 the MW field is quite uniform at that high Galactic latitude ($b=-89.38^\circ$), as judged by the small separation of the dotted horizontal lines to the solid line which represent the dispersion and mean values, respectively.

We then subtracted such a MW background level from the observed radial profile to derive that of NGC 288, which we overplotted with magenta symbols. Here, the errorbars come from considering in quadrature the MW field stellar density dispersion and that of the observed radial profile. For comparison purposes we superimposed the King (1962)'s and Plummer (1911)'s models with black and orange curves, respectively, using core (r_c), half-light (r_h) and tidal (r_t) radii derived by Miocchi et al. (2013). An Elson et al. (1987)'s model with the above r_c value and $\gamma = 3.9$ agrees pretty well with that of Plummer (1911). As can be seen, NGC 288 contains a population of extra-tidal stars reaching ~ 3.5 times its tidal radius.

At this point, it is not possible to assess whether that

extra-tidal structure reveals the existence of tidal tails. Indeed, some GGCs with a break in the radial density profiles – like the one observed in Fig 2 (left panel) – present tidal tails (e.g., Eridanus and Pal 15; Myeong et al. 2017), while others do not (e.g., NGC 1261 and NGC 7089; Kuzma et al. 2016, 2017). In order to address this issue, we investigated whether the resultant stellar density radial profile may vary with the orientation from the cluster centre. For that purpose, we repeated the above analysis distinguishing different position angles (PAs). We used angular sections of 45° and performed two star counts, one for stars closer than 120 pc (0.8°) from the cluster centre, and another for stars farther than that distance. We obtained the results shown in Fig. 2 (right panel). As can be seen, while the upper panel shows a variable stellar density as a function of the P.A., the lower panel suggests that the excess detected above the Plummer (1911)'s profile (see left panel of Fig. 2) is related to an excess of stars located towards the east of NGC 288 (central P.A. $\sim 90^\circ$). In the case of existing tidal tails, symmetrically collimated structures should have been detected well beyond the cluster body, which are not seen in the figure.

4 CMD CLEANING

Because we aim at disentangling very faint stellar structures in the surrounding region of NGC 288, the intrinsic stellar density map of the cluster must be built on the basis of cluster members distributed over the surveyed region. Fortunately, the cluster is located at a high Galactic latitude ($b=-89.38^\circ$) where variation of the MW field are mostly negligible (see Section 3).

In order to decontaminate the analysed area from the actual number of MW field stars at any particular position, we decided to clean the MS strip by statistically subtracting the MW stars that fall in that CMD region and that are located far from the cluster region, but not too far as to lose the local distribution in stellar density, magnitude and colour of MW stars. Notice that this approach is different from that based on a spatial filter analysis, and is advantageous because we dealt with intrinsic cluster CMD features (Olszewski et al. 2009; Piatti 2017a). The reference MW fields were chosen to be located to the north, east, south and west from the cluster, at a distance of 2.5 degree and with areas of $0.5^\circ \times 0.5^\circ$ each (see Table 1). From these regions, we built four CMDs and generated a sample of boxes ($g_o, (g-r)_o$) centred on each MW field star, with sizes ($\Delta(g), \Delta(g-r)$) defined in such a way that one of their corners coincides with the closest MW field star in that CMD. This procedure to map the MW field CMD was developed by Piatti & Bica (2012) and successfully used elsewhere (see, e.g. Piatti 2017b,a; Piatti et al. 2017). It has the advantage of accurately reproducing the reference star field in terms of stellar density, luminosity function and colour distribution.

Each of these four generated CMD box samples were superimposed to the CMDs of regions of $0.5^\circ \times 0.5^\circ$ distributed throughout the studied area around NGC 288 and subtracted from them one star per box; that closest to the box centre. The resultant cleaned CMD contains mainly cluster members, although some negligible amount of interlopers can be expected. Since we repeated this procedure four times, with reference MW fields strategically dis-

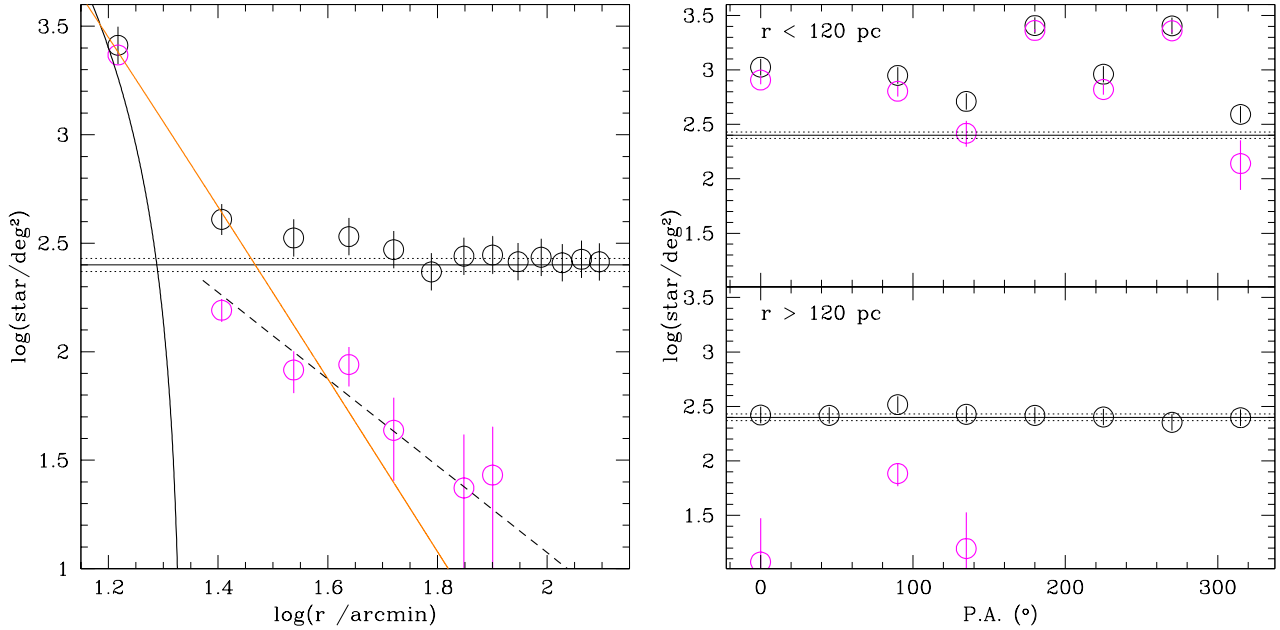


Figure 2. Left: Observed (black) and background subtracted (magenta) stellar density radial and profiles (open circles) with their respective errorbars. The horizontal lines represent the mean background level and its dispersion, while the curved black and orange lines are the King (1962)’s and Plummer (1911)’s models, respectively, with r_c , r_h and r_t taken from Miocchi et al. (2013). The dashed line represents a power law $\propto r^{-2}$. To convert angular to linear distances we used a cluster distance of 8.9 kpc (Harris 1996). Right: same profiles as a function of the P.A. for stars located closer and farther than 120 pc (0.8°) from the cluster centre.

tributed, we could assign photometric cluster membership by counting the number of times a star kept unsubtracted. Thus, stars subtracted three times have photometric membership probabilities $P = 25\%$, and mainly represent field populations projected on the cluster area; those subtracted two times, $P = 50\%$, which could indistinguishably belong to the field or to the cluster; those subtracted once, $P = 75\%$, i.e., stars that are predominantly found in the cluster rather than in the star field population, and those kept unsubtracted, $P = 100\%$. We generated stellar density maps of cluster members with $P = 25\%$, 50% , 75% and 100% , respectively. Such density maps are depicted in Fig. 3. Notice that stars with a statistical low probability of being cluster members ($P = 25\%$) do not trace any extended stellar structure around the cluster as that clearly visible in the $P = 100\%$ panel. There are small group of stars spread throughout the entire field. Particularly, an stellar excess located at (Relative R.A., Relative Dec.) $\approx (1.5^\circ, 0.5^\circ)$ – most clearly seen in the $P = 50\%$ panel – agrees with the excess observed in Fig. 2, namely, a stellar overdensity that contributes to the extended cluster stellar radial profile at distances larger than 120 pc from the cluster centre ($67.5^\circ \leq \text{P.A.} \leq 112.5^\circ$, centred at $\text{P.A.} = 90^\circ$).

We smoothed the star distribution with a $\sigma=3.6'$ Gaussian kernel, much smaller than the 16 arcmin of spatial resolution used by Leon et al. (2000). The resultant density map for $P = 100\%$ illustrates how the cluster density diminishes with increasing distances from its centre, and that a clumpy pattern with different mean densities are seen around it. It is in excellent agreement with the independent results found of Section 3, i.e., NGC 288 simply contains an extra-tidal structure; no long tidal tails oriented in the direction of the orbital motion (see proper motion vector in Fig. 3) as those

claimed by Leon et al. (2000) and Grillmair et al. (2004) could be uncovered. However, Montuori et al. (2007) and Klimontowski et al. (2009) have argued from N-body simulations that tidal tails near a cluster mainly point in the direction of the Galaxy centre (GC). For the sake of the reader Fig. 3 also illustrates the direction towards the GC. Seemingly, it is not straightforward to link such a direction with the stellar excesses. Nevertheless, some farther, few isolated small structures could be related to the cluster, if we considered stars with lower photometric membership probabilities.

5 ANALYSIS AND DISCUSSION

Our both independent approaches lead to conclude that NGC 288 is not a tidally limited GGC, but one with an extended structure that reaches ~ 3.5 times its tidal radius (Miocchi et al. 2013) and ~ 2.5 times its Jacobi radius ($r_J = 81.5$ pc Baumgardt et al. 2010). This could suggest that the cluster MS stars located in the outermost regions are experiencing, in some way, gravitational effects due to the MW potential. Tidal tails as those claimed by Leon et al. (2000, hereafter L00) and Grillmair et al. (2004, hereafter G04) have not been detected in this study.

In order to find some explanation for the present negative outcome we revisited the photographic CMD used by L00 (see their Figure 4). That figure barely reaches tenth of magnitudes below the cluster MSTO, with clear sign of photometry incompleteness (the darken the Hess diagram the more numerous the observed cluster star population along the cluster MS). The error quoted by L00 at $B \sim 20.0$ mag is Pan-STARRS PS1 data set $\sigma(B) \sim 0.2$ mag, which is nearly

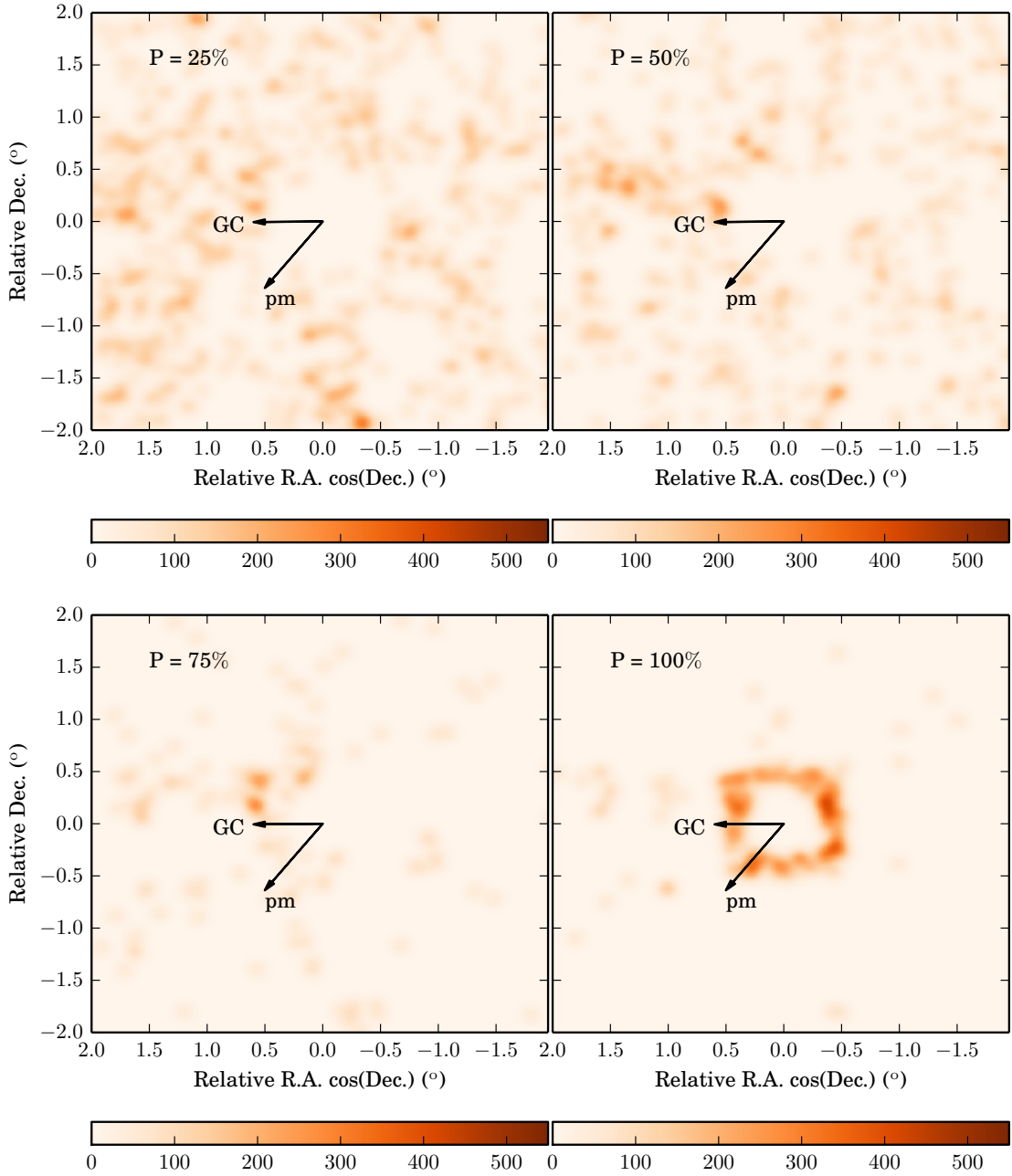


Figure 3. Stellar density maps with stars within different photometric membership probability ranges, as indicated at the top-left margin of each panel. The colourbars give the number of stars/deg². In order to highlight the outer cluster regions, we cut off stars located inside r_t . The arrows represent the cluster absolute proper motion vector (pm; [Dinescu et al. 1999](#); [Leon et al. 2000](#)) and that towards the Galactic centre (GC).

seven times larger than that in the Pan-STARRS PS1 data set used in the present work. On the other hand, L00 mentioned a not satisfactory background subtraction, with residuals of Abell galaxies that mimic cluster stellar excesses beyond the cluster main body. We think that these three main factors affected the final stellar density radial profile and stellar density map built by L00, and that the astrometric and photometric data set used here largely supersedes that previous photographic work. An additional difference

between L00 and the present results is the derived slope α for a power law $\propto r^{-\alpha}$ of the stellar density as a function of the distance to the cluster centre. While L00 obtained a value of 1.18, we derived $\alpha = 2$ (see dashed line in Fig. 2). Our value is in between those found in GGCs with extended halo-like structures, e.g., NGC 1851 and 47 Tuc ([Olszewski et al. 2009](#); [Piatti 2017a](#), $\alpha = 1.24$) and the abrupt fall of the r^{-4} law suggested by [Peñarrubia et al. \(2017\)](#) as a pre-

diction of expected stellar envelopes of GGCs embedded in dark mini-haloes.

G04's results are also hard to reproduce, namely, the existence of two main tidal tails of $\sim 8.5^\circ$ long that arise from the cluster centre towards to the north-west and south-east, respectively. One of both main tails have not been detected by L00, nor any of them in this work either. By revisiting the near-IR CMD used by G04 to claim such a detection (see their Figure 1), we realized that that 2MASS photometry does not reach the cluster MSTO, and that the CMD is largely more contaminated by MW field stars than its counterpart in the optical regime (see Fig. 1). Moreover, the cluster red giant and horizontal branches are so far no visible in that J versus $J - K$ CMD. Therefore, we are not aware of what CMD cluster features were traced by G04. All in all, both L00's photographic photometry and the Pan-STARRS PS1 data sets supersede that of 2MASS. Notice that GGCs with evidence of tidal tails show a symmetric density pattern (see, e.g., Odenkirchen et al. 2001; Belokurov et al. 2006; Niederste-Ostholt et al. 2010; Sollima et al. 2011; Balbinot et al. 2011; Erkal et al. 2017; Navarrete et al. 2017; Myeong et al. 2017), not distinguished in Fig. 3, either.

Our observational evidence about the extended structure of NGC 288 does not seem to be fully in the line of those argued from a theoretical point of view (Gnedin & Ostriker 1997; Dinescu et al. 1999; Balbinot & Gieles 2017), in the sense that disruption by tidal shocks were more important than internal relaxation and evaporation. Dinescu et al. (1999) listed eight GGCs (NGC 288, 5139, 6121, 6144, 6362, 6712, 6769 and Pal 5) with similar dynamics supporting the existence of tidal tails; only Pal 5 having been confirmed. According to recent works, NGC 5139 (Fernández-Trincado et al. 2015), NGC 6121 (Watkins & van der Marel 2017), NGC 4166, 6362, 6712 and 6779 (Chen & Chen 2010) do not show evidence of tidal tails. NGC 288, studied here, must now be included in this list, since the present outcomes suggest that Galactic tidal interaction has been a relatively inefficient process for stripping stars off the cluster. At this point it would be interesting to derive accurate GGC proper motions, for instance, from the next Gaia Data Release 2 (DR2) and to compute again their orbital motions and, on the other hand, to derive stellar radial profiles in an homogeneous scale. Thus, it would be possible to search for any relationship between extended structural features and orbital motions as to infer whether GGC masses, or the number of passages near the Galactic centre, or any other orbital parameter (e.g., eccentricity, inclination), or their birthplaces have to deal with the structural features seen far away the clusters' centres.

6 CONCLUSIONS

The issue about the extended structures of GGCs has fueled a renewed debate with the advent of large photometric surveys that allow us to cover homogeneously wider areas and analysed them from deep photometry. GGCs show a wide variety of extended structures, from those having no signature for such a feature to those with long tidal tails, passing through those exhibiting extra-tidal stellar populations more or less extended, azimuthally distributed or as clumpy features. Up-to-date, there is not a clear consensus

for their origins and contradict results have been published for some of them.

Here we performed a sound analysis of the external region around NGC 288, claimed by L00 and G04 to have visible tidal tails, and supported by studies of its orbital motion as a very good candidate to have long tidal tails. For this purpose, we took advantage of the Pan-STARRS PS1 data set for an area of $4^\circ \times 4^\circ$ around the cluster. From the cluster CMD we defined a strip along the cluster MS where we carried out stars count in order to construct the cluster stellar density radial profile and a stellar density map.

The MW subtracted stellar density radial profile shows an extra-tidal population of cluster stars that extends up to ~ 3.5 times the cluster tidal radius. This is a moderate extended structure, since other GGCs show evidence of such a features up to nearly more than 6 times their tidal radii (e.g., NGC 1851, 47 Tuc). The stellar density map built with stars that have photometric membership probabilities equal or higher than 50 per cent reveals a somehow clumpy structure around the cluster with different stellar densities, in excellent agreement with the resultant radial profile. The detected extra-tidal component is well matched by a power law with $\alpha = 2$. None of both independent approaches shed light on the possibility of the existence of tidal tails. This points to the need of more reliable orbital motions in order to constrain whether the number of passages near the Galactic centre, the eccentricity, the birthplaces, the masses, among other parameters are responsible for the wide variety of extended GGC's features seen until the present.

ACKNOWLEDGEMENTS

We thank C. Grillmair and D. Casetti-Dinescu for reading the manuscript and making fruitful comments, and the referee for the thorough reading of the manuscript and timely suggestions to improve it.

REFERENCES

- Balbinot E., Gieles M., 2017, preprint, ([arXiv:1702.02543](https://arxiv.org/abs/1702.02543))
 Balbinot E., Santiago B. X., da Costa L. N., Makler M., Maia M. A. G., 2011, *MNRAS*, **416**, 393
 Baumgardt H., Parmentier G., Gieles M., Vesperini E., 2010, *MNRAS*, **401**, 1832
 Belokurov V., Evans N. W., Irwin M. J., Hewett P. C., Wilkinson M. I., 2006, *ApJ*, **637**, L29
 Carballo-Bello J. A., Gieles M., Sollima A., Koposov S., Martínez-Delgado D., Peñarrubia J., 2012, *MNRAS*, **419**, 14
 Chambers K. C., et al., 2016, preprint, ([arXiv:1612.05560](https://arxiv.org/abs/1612.05560))
 Chen C. W., Chen W. P., 2010, *ApJ*, **721**, 1790
 Correnti M., Bellazzini M., Dalessandro E., Mucciarelli A., Monaco L., Catelan M., 2011, *MNRAS*, **417**, 2411
 Dinescu D. I., Girard T. M., van Altena W. F., Mendez R. A., Lopez C. E., 1997, *AJ*, **114**, 1014
 Dinescu D. I., Girard T. M., van Altena W. F., 1999, *AJ*, **117**, 1792
 Elson R. A. W., Fall S. M., Freeman K. C., 1987, *ApJ*, **323**, 54
 Erkal D., Koposov S. E., Belokurov V., 2017, *MNRAS*, **470**, 60
 Fernández-Trincado J. G., Vivas A. K., Mateu C. E., Zinn R., Robin A. C., Valenzuela O., Moreno E., Pichardo B., 2015, *A&A*, **574**, A15
 Gnedin O. Y., Ostriker J. P., 1997, *ApJ*, **474**, 223

- Grillmair C. J., Freeman K. C., Irwin M., Quinn P. J., 1995, *AJ*, **109**, 2553
- Grillmair C. J., Jarrett T. H., Ha A. C., 2004, in Prada F., Martínez Delgado D., Mahoney T. J., eds, *Astronomical Society of the Pacific Conference Series Vol. 327, Satellites and Tidal Streams*. p. 276
- Harris W. E., 1996, *AJ*, **112**, 1487
- Hozumi S., Burkert A., 2015, *MNRAS*, **446**, 3100
- King I., 1962, *AJ*, **67**, 471
- Klimentowski J., Lokas E. L., Kazantzidis S., Mayer L., Mamon G. A., Prada F., 2009, *MNRAS*, **400**, 2162
- Küpper A. H. W., Kroupa P., Baumgardt H., Heggie D. C., 2010, *MNRAS*, **401**, 105
- Kuzma P. B., Da Costa G. S., Mackey A. D., Roderick T. A., 2016, *MNRAS*, **461**, 3639
- Kuzma P. B., Da Costa G. S., Mackey A. D., 2017, preprint, ([arXiv:1709.02915](https://arxiv.org/abs/1709.02915))
- Leon S., Meylan G., Combes F., 2000, *A&A*, **359**, 907
- Miocchi P., et al., 2013, *ApJ*, **774**, 151
- Montuori M., Capuzzo-Dolcetta R., Di Matteo P., Lepinette A., Miocchi P., 2007, *ApJ*, **659**, 1212
- Myeong G. C., Jerjen H., Mackey D., Da Costa G. S., 2017, *ApJ*, **840**, L25
- Navarrete C., Belokurov V., Kozlov S. E., 2017, *ApJ*, **841**, L23
- Niederste-Ostholt M., Belokurov V., Evans N. W., Kozlov S., Gieles M., Irwin M. J., 2010, *MNRAS*, **408**, L66
- Odenkirchen M., et al., 2001, *ApJ*, **548**, L165
- Odenkirchen M., et al., 2003, *AJ*, **126**, 2385
- Olszewski E. W., Saha A., Knezek P., Subramaniam A., de Boer T., Seitzer P., 2009, *AJ*, **138**, 1570
- Peñarrubia J., Varri A. L., Breen P. G., Ferguson A. M. N., Sánchez-Janssen R., 2017, preprint, ([arXiv:1706.02710](https://arxiv.org/abs/1706.02710))
- Piatti A. E., 2017a, preprint, ([arXiv:1708.06194](https://arxiv.org/abs/1708.06194))
- Piatti A. E., 2017b, *MNRAS*, **465**, 2748
- Piatti A. E., Bica E., 2012, *MNRAS*, **425**, 3085
- Piatti A. E., Cole A., Emptage B., 2017, *MNRAS*.
- Plummer H. C., 1911, *MNRAS*, **71**, 460
- Saha A., et al., 2010, *AJ*, **140**, 1719
- Schlafly E. F., Finkbeiner D. P., 2011, *ApJ*, **737**, 103
- Schlegel D. J., Finkbeiner D. P., Davis M., 1998, *ApJ*, **500**, 525
- Sollima A., Martínez-Delgado D., Valls-Gabaud D., Peñarrubia J., 2011, *ApJ*, **726**, 47
- Trager S. C., Djorgovski S., King I. R., 1993, in Djorgovski S. G., Meylan G., eds, *Astronomical Society of the Pacific Conference Series Vol. 50, Structure and Dynamics of Globular Clusters*. p. 347
- Watkins L. L., van der Marel R. P., 2017, *ApJ*, **839**, 89

This paper has been typeset from a $\text{\TeX}/\text{\LaTeX}$ file prepared by the author.